JCTC Journal of Chemical Theory and Computation

Gold(I)-Catalyzed Hydration of 1,2-Diphenylacetylene: Computational Insights

Gloria Mazzone, Nino Russo, and Emilia Sicilia*

Dipartimento di Chimica, Università della Calabria, I-87030, Arcavacata di Rende, Italy

Received May 14, 2010

Abstract: A DFT investigation of 1,2-diphenylacetilene hydration mediated by the $[(Ph_3P)Au]^+$ complex has been carried out to shed light on the mechanistic details of such process with the support of the experimental observations and mechanistic proposal. Computational analysis proves that the first inner-sphere attack of water occurs with gold acting as a proton shuttle to transfer the migrating hydrogen in cis position with respect to OH group. From the formed *E* isomer of the enol the *Z* one could be formed by rotation around the C−C bond. The addition of the second water molecule to give the ketone final product occurs favorably with the assistance of the catalyst and involves coordination of water followed by a second hydrogen shift from oxygen to carbon. If the *E* isomer is involved, gold directly participates in the reaction assisting the hydrogen transfer, whereas if the product is obtained starting from the *Z* isomer, gold is not directly involved. The elimination of a water molecule and the release of the catalyst close the catalytic cycle. Calculations show that the intervention of a third water molecule lowers the energy barrier for the elimination of water and formation of the π carbonyl bond.

1. Introduction

The hydration of unsatured carbon compounds is one of the most environmentally benign and economically attractive route to form a carbon−oxygen bond. Unactivated alkynes are an abundant hydrocarbon resource and hydration represents an excellent means of functionalization, which has been extensively studied.[1−5]

It has long been known that water can be added quite easily to activated electron-rich alkynes in the presence of an acid catalyst.[6,7] The reaction of simple alkynes, instead, needs cocatalysts, typically mercury(II) salts, to enhance the reactivity.[8−14] Such catalysts have been extensively used in high-scale industrial processes[15] until the discovery of the toxicity of mercury salts. Moreover, under the reaction conditions the mercury(II) is quickly reduced to catalytically inactive metallic mercury. To avoid the use of toxic mercury salts there has been much effort aimed at the development of alternative synthetic strategies for the hydration of alkynes based on the use of metal catalytic systems,[16] but neither of them has shown activity comparable to that of those mercury salt containing systems. Among the alternative systems, gold compounds have gradually taken a prominent place, beneficially replacing mercury salts. A notable landmark in the application of gold in this field is the report, after 90 years, of Teles and co-workers, in which the addition of methanol to alkynes has been reported to be efficiently catalyzed by coordinatively unsaturated cationic gold(I) species, of the type R_3PAu^+, generated in situ by the protonolysis of R_3PAuCH_3 with an acid and release of CH_4.[17,18] A remarkable result of Teles work stems from theoretical calculations for the reaction pathway that show how gold(I) directs the alcohol nucleophile to the side of the coordinated metal. This behavior is different from the usual attack of the nucleophile from the side opposite to the coordinated metal that is assumed for other electrophilic metals. In 2002, Tanaka et al. using similar reagents achieved the efficient hydration of a wide range of alkynes in aqueous methanol.[18] Good yields have been reported also by Laguna[19] and others,[20] especially when gold(I) complexes were combined with strong acids under heating. Very recently, Leyva and Corma have carried out the efficient hydration of a wide range of alkynes to the corresponding ketones by using gold(I)−phosphine complexes as catalyst with no acidic cocatalyst.[21]

* To whom correspondence should be addressed. E-mail: siciliae@unical.it.

10.1021/ct100254v
Published on Web 08/03/2010

Scheme 1. Proposed Catalytic Cycle for the Alkynes Hydration in Presence of $AuPR_3^+$ Catalysts

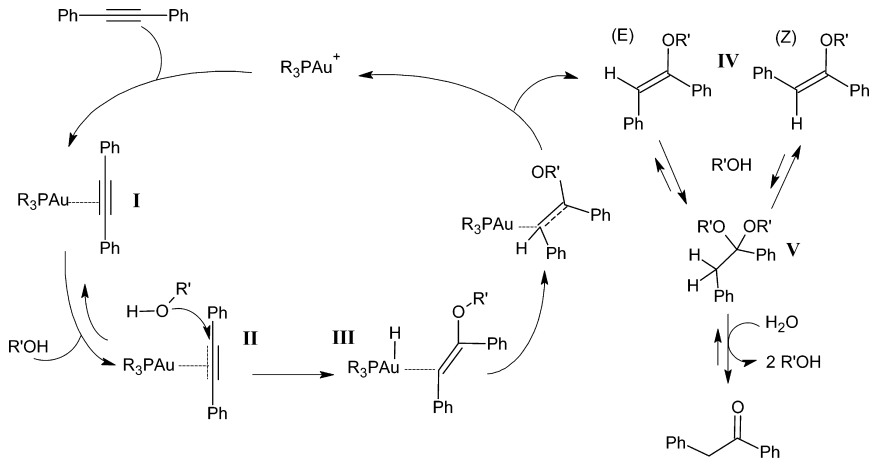

Catalysts like R_3PAuX (X = trifluoromethanesulfonate $^-$OTf or other weakly coordinating counteranions) have been formed in situ by treatment of the corresponding chloride complex, R_3PAuCl, with a silver salt. The soft noncoordinating anions make the catalytic center acidic enough to bypass the use of additives. To shed light on the proposed mechanistic hypotheses,[17−19] even contradictory, for this reaction the authors have carried out a series of kinetic experiments using H_2O, MeOH, or both as nucleophiles; 1,2-diphenylacetylene as substrate; and $AuPR_3X$ (PR_3 = PPh_3, SPhos, P^tBu_3; X = Cl, OTf, NTf_2) as catalyst in THF solvent.

The mechanism proposed by the authors on the basis of experimental findings involves (Scheme 1) coordination of the triple bond to Au(I) complex with formation of the Au−π-alkyne complex **I** and subsequent attack of the R′OH (R′ = H, CH_3) nucleophile. R′OH would coordinate to gold, leading to formation of the intermediate **II**, before its addition to the triple bond (**III**) to afford, by protodeauration, the *E* isomer of the enol ether product **IV** together with the restored catalyst. Formation of the *Z* from the *E* isomer can occur by rotation about the C−C double bond[17] or in the next step of the overall process, that is, addition of a second molecule of R′OH to form the corresponding ketal **V**. Elimination of a R′H molecule from the **V** would explain formation of both *Z* and *E* isomers, whereas subsequent reaction of ketal **V** with H_2O leads to the formation of the ketone final product. The authors suggest that the gold catalyst could come into play also in these last steps of the overall hydration process.

As the first step of a more comprehensive project, we have investigated here, with the aid of density functional theory (DFT) calculations, the detailed mechanism of the whole of 1,2-diphenylacetylene hydration process catalyzed by the gold(I) $[(Ph_3P)Au]^+$ complex using pure water as nucleophile with the support of the experimental observations and mechanistic proposal. The water is able to attack the alkyne from the same side of the coordinated catalyst (inner-sphere mechanism) or from the opposite side (outer-sphere mechanism). Even if not envisaged by Teles and Leyva and Corma, the outer-sphere attack of H_2O to the alkyne has been also explored.

The theoretical insights presented in this work are expected to be helpful in understanding such kind of gold-catalyzed hydration reactions and provide helpful information for chemists on similar processes.

2. Computational Details

All molecular geometries have been optimized at the Becke3-LYP (B3LYP) level of density functional theory.[22,23] Numerous theoretical studies of Au-catalyzed reactions at the B3LYP level have been reported in the literature, which confirm that such exchange-correlation functional is quite suitable to investigate Au-catalyzed reactions.[24−27] However, to check the effect of the exchange-correlation functional, additional calculations employing the B97-1[28] functional have been carried out. B97-1 functional, indeed, has been shown by Zhao and Truhlar to provide energetics of comparable quality to MP2 results for weakly interacting systems.[29]

For both B3LYP and B97-1 functionals, frequency calculations at the same level of theory have been also performed to identify all stationary points as minima (zero imaginary frequencies) or transition states (one imaginary frequency).

The transition states involved have been checked by IRC (intrinsic reaction coordinate) analysis.[30,31] For Au, the relativistic compact Stuttgart/Dresden effective core potential[32] has been used in conjunction with its split valence basis set. In order to reduce the computational cost of stationary points, optimization standard 6-31G basis set of Pople for carbon and hydrogen atoms of phenyl rings has been used together with the 6-31G** for the rest of the atoms. Final energies have been calculated by performing single-point calculations on the optimized geometries at the same level of theory and employing 6-311+G** standard basis sets for H, C, O and P atoms. All the calculations have been performed with the Gaussian 03 software package.[33]

The impact of solvation effects on the energy profiles has been estimated by using the conductor polarizable continuum model (CPCM)[34] as implemented in Gaussian 03. The UAHF set of radii has been used to build up the cavity. Since preliminary calculations have clearly shown geometry relaxation effects to be not significant, the solvation Gibbs free energies have been calculated in implicit THF (ε = 7.58), the solvent medium in the experiments, with the above

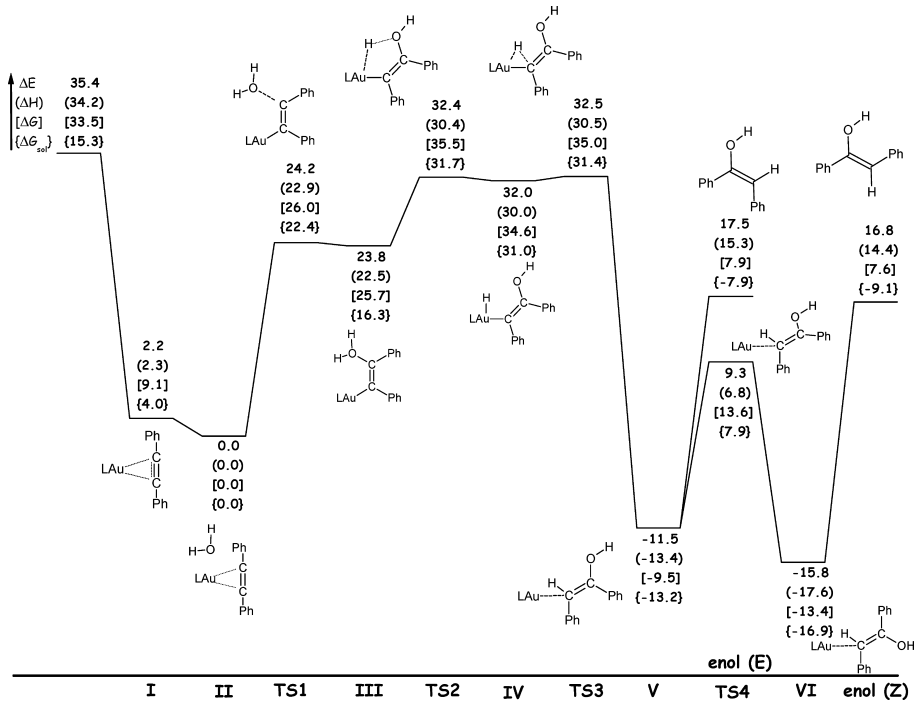

Figure 1. Calculated B3LYP PES for the addition of the first water molecule to 1,2-diphenylacetilene catalyzed by the gold(I) $[(Ph_3P)Au]^+$ complex. Relative ZPE-corrected electronic energies, enthalpies, and Gibbs free energies at 298.15 K together with free energy changes in THF are reported. Relative energies are in kcal/mol.

method performing single-point calculations on all stationary points structures obtained from vacuum calculations at the B3LYP level. Other authors also have observed the negligible influence of solute geometry relaxation in solution.[35−37] Reaction Gibbs free energies in solution, ΔG_{sol}, have been calculated for each process as the sum of two contributions: a gas-phase reaction free energy, ΔG_{gas}, and a solvation reaction free energy term calculated with the continuum approach, ΔG_{solv}. Single point energies have been also computed at the MP2 level through the RI-MP2[38] approach as implemented in the TURBOMOLE program package[39] (version 5.10) in conjunction with the same relativistic Stuttgart/Dresden pseudopotential for gold and the standard internally stored TZVP basis set[40,41] for the rest of the atoms (see Figures S1 and S2 of the Supporting Information).

3. Results and Discussion

3.1. First H_2O Molecule Addition. B3LYP and B97-1 calculated energy profiles for the reaction pathway corresponding to the addition of the first H_2O molecule are shown in Figure 1 and Figure S3 of Supporting Information, respectively. Relative ZPE corrected electronic energies (ΔE), enthalpies (ΔH), and Gibbs free energies (ΔG) at 298 K, as well as free energies in THF (ΔG_{sol}) are provided. Unless otherwise noted, in what follows, the discussed energies are B3LYP-relative ZPE-corrected electronic energies calculated with respect to the intermediate named **II**.

Structures of reactants, intermediates, transition states, and products of the reactions are schematically depicted in the same figure. Fully optimized B3LYP and B97-1 structures of stationary points can be found in Figures S6 and S7 of the Supporting Information, respectively.

From the energy profiles in Figure 1, it is evident that the first step along the pathway for the catalytic addition of water to the alkyne involves a preliminary intermediate, **I**, where the C−C triple bond interacts with the gold atom. Intermediate **I** is formed without any barrier and is 33.2 kcal/mol lower in energy than $[(Ph_3P)Au]^+ + C_2Ph_2 + H_2O$ reactants. Several examples[42−46] of such a π-coordination to gold(I) have been theoretically studied to evaluate the extent of the π-to-metal σ-donation and metal-to-π^* back-donation, and the main conclusion is that Au(I) cation cannot significantly participate to a Dewar−Chatt−Duncanson-type bonding,[47,48] as antibonding orbitals are too high in energy for significant back-bonding to occur. Here the C1−C2 bond has lost a little of its triple bond character. Indeed, the C−C length increases from 1.205 Å, calculated for the free alkyne, to 1.239 Å, and the deviation from linearity is measured by the value of 169.5° of the C1−C2−C4 angle. With these optimized geometries in hand, the natural bond order (NBO)[49,50] analysis have been used to investigate the nature of the metal−alkyne bond. Second-order perturbative analysis has revealed that π-to-metal σ-donation largely dominates (105.8 kcal/mol) over metal-to-π^* back-donation (14.1 kcal/mol). In addition to NBO analysis also the frontier molecular orbitals have been examined (see Figure 2). As expected, the LUMO contains the π^*−metal interaction. Furthermore, results from the calculation of the energies of the frontier orbitals of the two species $[(Ph_3P)Au]^+$ and C_2Ph_2 show that the HOMO of diphenylacetylene is only 0.3 eV higher in energy than the LUMO of the gold(I) complex. The difference in energy, instead, between the HOMO of $[(Ph_3P)Au]^+$ and the LUMO of C_2Ph_2 is very large, that is, 9.4 eV. The lack of back-bonding from Au(I) enhances the electrophilicity of the ligand and favors the attack of the

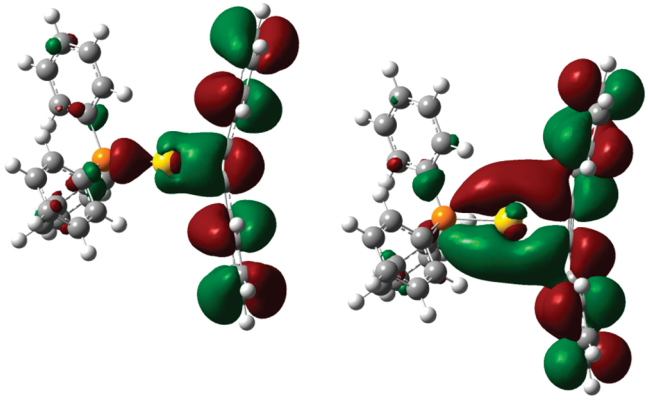

Figure 2. Structure of the highest occupied and lowest unoccupied molecular orbitals of the $[(Ph_3P)Au\text{-alkyne}]^+$ complex.

nucleophile. As a first step, the intermediate **II** is formed in which water is loosely coordinated to the metal. This precoordination is computed to be exothermic by 2.2 kcal/mol and introduces some changes into the structure of the complex. The lengths of the two Au−C bonds, that are 2.332 Å, become different (Au−C1 = 2.356 Å and Au−C2 = 2.306 Å). The angle between phosphorus, gold, and the next C2 carbon of the triple bond changes from 164.3° to 156.9°. The Au−O bond is 3.039 Å and the P−Au−O angle is 82.9°.

The next step involves formation of intermediate **III** by coordination between the O-atom of water and one carbon atom of the diphenylacetylene concomitant with a movement of Au^+ to the other carbon. The calculated activation energy for rearrangement of **II** to **III** is 24.2 kcal/mol, and the intermediate **III** is only slightly more stable than the transition state leading to it. The further reaction toward formation of the *E* isomer of the enol coordinated to the Au(I)-complex involves an Au^+-assisted hydrogen migration from oxygen, via gold, to the terminal carbon to finally afford the product complex **V** with a relative energy of −11.5 kcal/mol. The first step, that is, migration to Au^+, has a computed activation energy of 8.6 kcal/mol, and the intermediate **IV** is formed that lies 32 kcal/mol higher in energy with respect to reference adduct **II**. The next hydrogen shift from gold to the position cis to the OH group corresponds to a very low activation energy of about 0.5 kcal/mol. Even if the very small differences in energy among the **TS2** and **TS3** transition states and **IV** intermediate could suggest the involvement of a concerted rearrangement, all the attempts to intercept a transition state directly connecting **III** and **V** intermediates have been unsuccessful. MP2 calculations (see Figure S1 of the Supporting Information) confirm this result.

Our calculations show that the *Z* isomer formation occurs exclusively by rotation around the C−C double bond of the complex **V**, since no pathway exists for the direct transfer of the hydrogen atom from oxygen to the position trans to the OH group. The transition state structure for the catalyst-assisted *E* to *Z* isomerization is located at a relative energy of 9.3 kcal/mol and corresponds to an activation energy of 20.8 kcal/mol, which is significantly lower than the barrier to rotation around a double bond in the absence of catalyst, both experimentally and theoretically estimated to be approximately 65 kcal/mol.[51,52]

The *Z* isomer coordinated to the gold complex is stabilized by 4.3 kcal/mol with respect to the *E* one. As pointed out in recent literature,[53,54] even if gold−alkene π-complexes are known for a long time, the number of such structurally characterized complexes is quite limited. From our computational analysis results, for both isomers the binding of Au^+ to the double bond is very asymmetric in that the gold atom is only attached to the C2 terminal carbon atom. The C1−C2 bond length is 1.402 Å for the *E* isomer and 1.398 Å for the *Z* isomer. The C1−C2−Au angle amounts to 90.7° and 89.7° in *E* and *Z* isomers, respectively. NBO analysis reveals that even if π-to-metal σ-donation plays a role, electrostatic interactions are the primary origins of the bond. Both NBO and ESP[55,56] charge analyses show that the positive charge is significantly redistributed on the ligand and the gold atom carries a charge not larger than 0.29. An attractive interaction, therefore, exists with the C2 atom of the alkene that carries a negative charge, whereas the C1 atom is positively charged due to the bond with the O atom. More details can be found in Figure S8 of the Supporting Information. The catalytic cycle could be, then, closed, either by the *Z* isomer of the enol release that is calculated to be endothermic by 32.6 kcal/mol or by the loss of the *E* isomer that requires 29 kcal/mol to occur.

To close this section concerning the addition of the first water molecule, we report the results obtained by the investigation of the outer-sphere mechanism. Figure 3 presents the B3LYP energy profile for the water attack from the opposite side with respect of the coordinated catalyst, whereas selected geometrical parameters of stationary points are shown in Figure S9 of Supporting Information.

Once the preliminary intermediate **I** is formed, further stabilization is due to the loose precoordination of the water molecule that weakly interacts with one of the triple bond carbon atoms. This step, calculated to be the exothermic by 3.1 kcal/mol, is followed by the simultaneous formation of the C1−O bond and the cleavage of one O−H bond, accompanied by the transfer of the hydrogen atom to the C2 atom. This rearrangement, corresponding to the formation of the **TS1′** transition state, has a very high energetic cost of 60.6 kcal/mol and leads to the formation of the *E* isomer of the enol coordinated to catalyst. It is worth noting that the **TS1′** transition state rearrangement involves the coordination of the gold catalyst to the carbon atom of the C1−C2 alkene bond being replaced by the interaction of the gold atom with one of the phenyl rings of the alkyne. Therefore, to obtain the final complex **V** it is necessary to overcome a low energy barrier, of 4.4 kcal/mol, corresponding to the transition state, **TS2′**, which allows gold to restore the initial coordination to the C−C bond of the alkene. On the basis of the very high energy barrier calculated along the outer-sphere nucleophilic attack pathway, these results strongly support an inner-sphere mechanism.

3.2. Second H_2O Molecule Addition. As underlined by the authors,[21] the catalyst could play also a role in the next steps of the whole process that involves the addition of a second water molecule. To evaluate which is the most favorable pathway, we have calculated the energy profiles for the reaction occurring both in the absence of and assisted

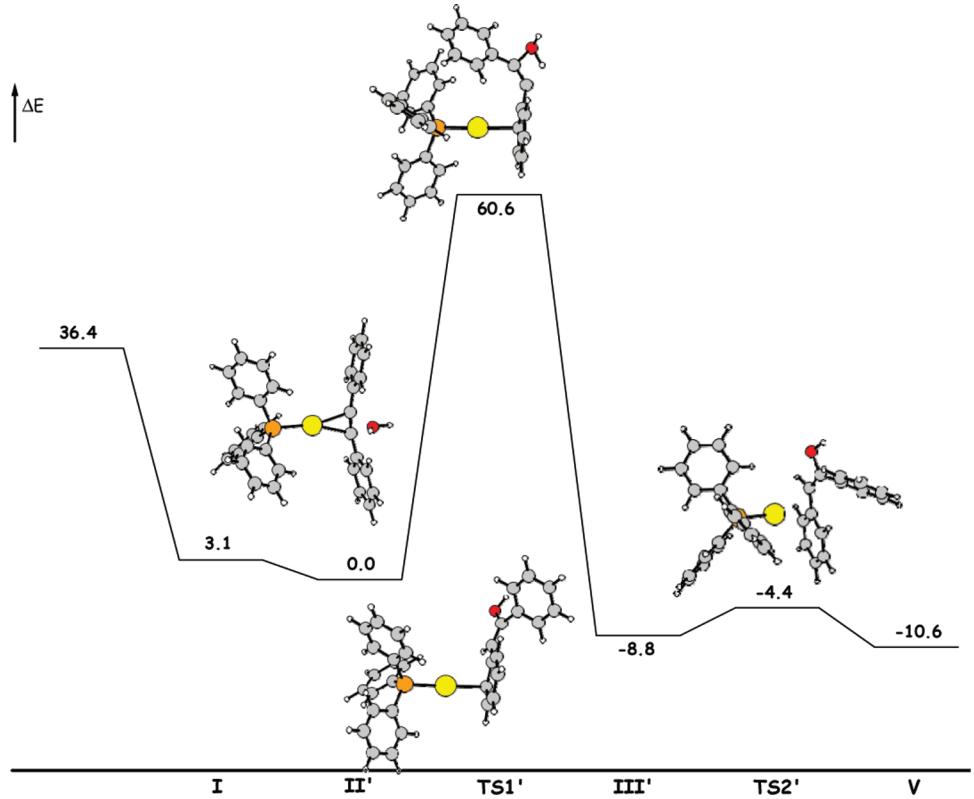

Figure 3. Calculated B3LYP energy profile for the outher-sphere attack of the first water molecule to 1,2-diphenylacetilene catalyzed by the gold(I) $[(Ph_3P)Au]^+$ complex. Relative ZPE-corrected electronic energies, in kcal/mol, are reported.

by the gold catalyst. B3LYP- and B97-1-calculated energy profiles for the reaction pathway corresponding to the addition of the second water molecule are shown in Figure 4 and Figure S4 of Supporting Information, respectively. We are going to comment only on B3LYP-relative ZPE-corrected electronic energies (ΔE), calculated with respect to the **II** intermediate, even if also enthalpies (ΔH) and Gibbs free energies (ΔG) at 298 K as well as free energies in THF (ΔG_{sol}) have been calculated and reported. In the same Figure 4, the B3LYP energy profile for the direct addition of water in the absence of the gold catalyst is also shown (see Figure S10 of the Supporting Information for more details). Fully optimized B3LYP and B97-1 structures of stationary points intercepted along the catalyst-assisted reaction pathway can be found in Figures S11 and S12 of Supporting Information, respectively.

Along the catalyst-assisted pathway both **V** and **VI** adducts, that is, *E* and *Z* isomers coordinated to the $[(Ph_3P)Au]^+$ complex, can enter the subsequent catalytic cycle for the addition of a second water molecule. Indeed, the possibility that the isomerization from *E* to *Z* isomers occurs depends on how rapidly the final ketone product is formed. For that reason, we have investigated the pathway for the addition of a second H_2O molecule starting from both **V** (solid line in Figure 4) and **VI** (dashed line in Figure 4) intermediates.

The B3LYP-calculated energy profiles in Figure 4 show that the first step of the process is the loose coordination of H_2O that is calculated to be exothermic by 19.8 kcal/mol and 25.7 with respect to **II** intermediate along *E* and *Z* enol isomers pathways, respectively. An examination of Figure 4 shows that along the path involving the *E* isomer the reaction proceeds by a 1,3-hydrogen migration with gold acting as a proton shuttle. Oxygen coordinates to C2 and one of the hydrogen atoms is transferred to Au to form the **VIIIa** intermediate that lies 28.5 kcal/mol above the energy of **II** intermediate. The barrier for this rearrangement (**TS5a**) is 48.8 kcal/mol, whereas the barrier for the next hydrogen shift from Au to the carbon atom (**TS6a**) to form the corresponding *gem*-diol **IX** is very low and amounts to 1.0 kcal/mol. Although on the basis of the flatness of the PES in this region one can suspect that the reaction occurs in one step, B97-1 analysis, as well as MP2 computations (see Figure S2 of Supporting Information), confirm the existence of two distinct transition states and of the minimum between them. Along the *Z* isomer pathway, instead, the intermediate **IX** formation takes place directly (**TS5b**), since the hydrogen atom is transferred from oxygen to carbon in one step and the barrier that is necessary to overcome is 55.2 kcal/mol. Therefore, the calculated barrier for the *E* to *Z* isomerization (first H_2O molecule addition) is lower than both the barrier that must be overcome to generate from the *E* isomer the **IX** intermediate and the reverse barrier to go from **IX** to the *Z* isomer by elimination of a water molecule (45.9 kcal/mol). Hence, it should be concluded that formation of the Z isomer is likely to occur by direct isomerization from the *E* isomer. The final step of the reaction, that is, formation of the ketone product from intermediate **IX**, can occur both by direct elimination of a water molecule from the two OH groups and by the involvement of a third molecule of water. The transition states for the both pathways have been intercepted. In Figure 5 are reported the B3LYP energetics of the process involving an additional water molecule assisting the elimination reaction, leading to formation of the ketone coordinated

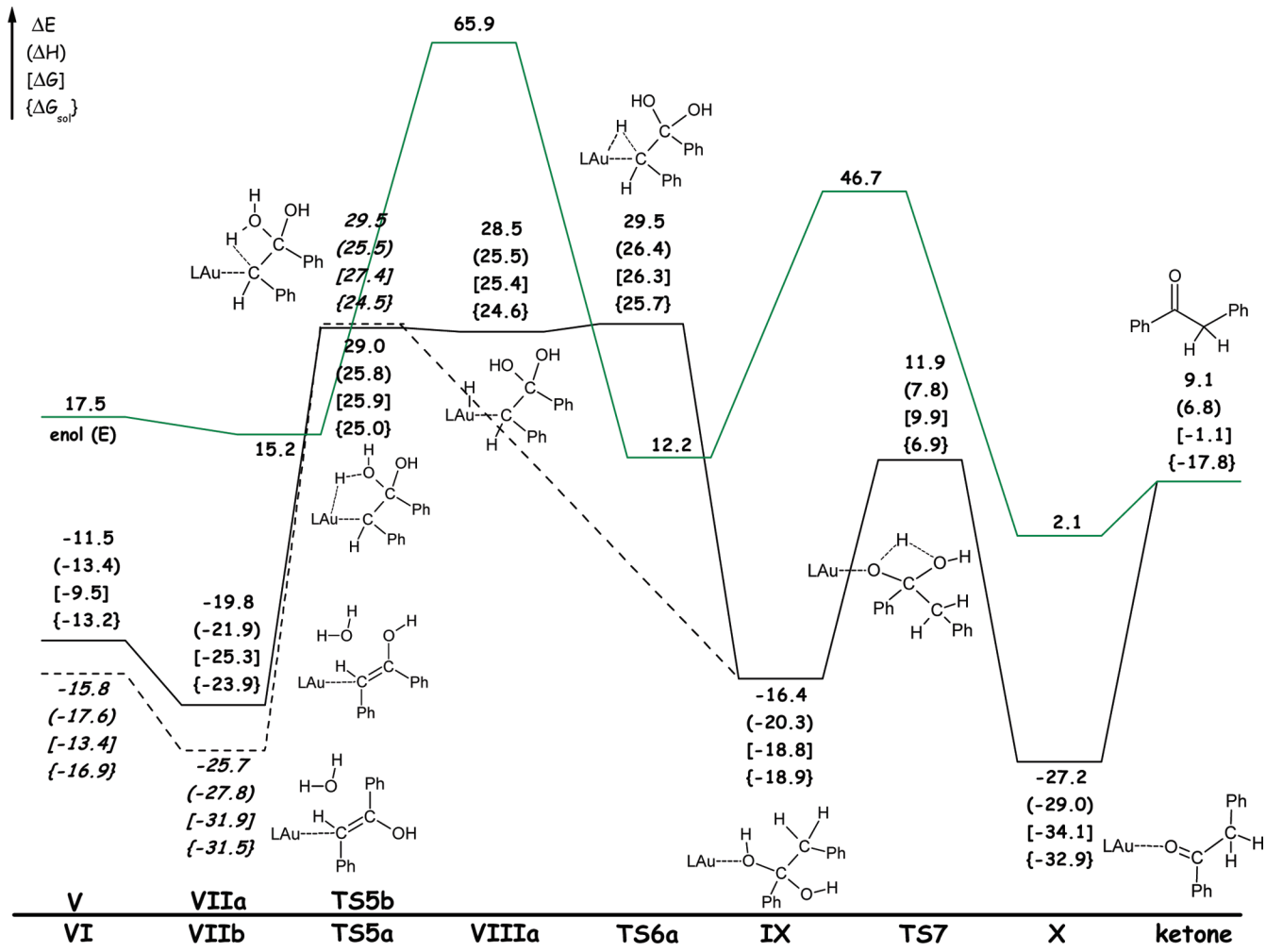

Figure 4. Calculated B3LYP energy profiles for the addition of the second water molecule to enol *E* (solid line) and *Z* (dashed line) isomers coordinated to the $[(Ph_3P)Au]^+$ complex. Relative ZPE-corrected electronic energies (ΔE), enthalpies (ΔH), and Gibbs free energies (ΔG) at 298.15 K together with free energy changes in THF (ΔG_{sol}) are reported. The energetics of the uncatalyzed pathways is also reported (green line). Relative energies are in kcal/mol.

yet to the catalyst. The same energetics explored with the B97-1 functional can be found in Figure S5 of the Supporting Information. B3LYP and B97-1 geometrical structures of involved stationary points are included in Figures S11 and S12, respectively.

As can be clearly inferred from the comparison between Figures 4 and 5, the process is calculated to be more favorable if the participation of a third water molecule is taken into consideration. The elimination of a water molecule directly from the intermediate **IX** occurs through the **TS7** transition state, whose formation is endothermic by 11.9 kcal/mol relative to the reference energy of the intermediate **II** and the corresponding activation barrier amounts to 28.3 kcal/mol. As a result of a hydrogen shift from one oxygen to the other, a water molecule is eliminated and the carbonyl bond is formed (minimum **X**). The **TS7′** transition state, instead, lies at 7.8 kcal/mol below the reference energy of **II** and corresponds to a barrier of 8.6 kcal/mol. The calculated imaginary frequency is associated with the movement of the third water molecule that approaches the complex and induces formation of the product by abstracting a hydrogen atom from one of the two OH groups and simultaneously transferring a hydrogen atom to the other OH. The formation of the adduct **X′** with two directly interacting H_2O molecules is calculated to be slightly more exothermic than the formation of the **X** adduct with one water molecule, 30.7 kcal/mol versus 27.2 kcal/mol. To release the product and to regenerate the catalyst require overcoming an energy barrier of 36.3 and 39.8 kcal/mol from intermediate **X** and **X′**, respectively. The whole catalytic process is endothermic by 9.1 kcal/mol if intermediate **II** is assumed to be the reference, whereas with respect to $[(Ph_3P)Au]^+ + C_2Ph_2 + H_2O$ starting reactants the whole process is exothermic by 26.3 kcal/mol. Comparison in Figure 4 of the catalyzed and uncatalyzed pathways clearly shows that the intervention of the catalyst also in the second part of the process is crucial to lower the energy barriers and to act in such a way that all the stationary points along the reaction path lie below the energy of the reactants asymptote.

4. Conclusions

The investigation of the whole hydration process of 1,2-diphenylacetylene catalyzed by the gold(I) $[(Ph_3P)Au]^+$ complex by addition of water to form the corresponding ketone has been carried out and the mechanistic hypoth-

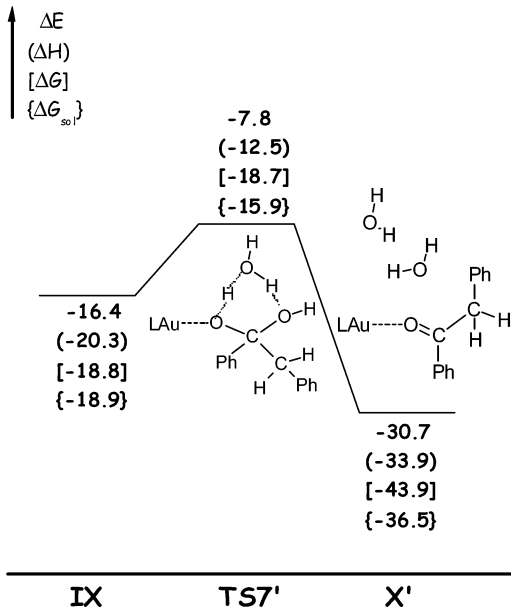

Figure 5. Calculated B3LYP energy profile for the water elimination step, leading to formation of the ketone coordinated to the catalyst, assisted by a third H_2O molecule. Relative ZPE-corrected electronic energies (ΔE), enthalpies (ΔH), and Gibbs free energies (ΔG) at 298.15 K together with free energy changes in THF (ΔG_{sol}) are reported. Energies are in kcal/mol and relative to intermediate **II**.

eses existing in the literature have been explored. In total, we can summarize our findings as follows. Calculations confirm that the first molecule addition occurs with gold acting as a proton shuttle to transfer the migrating hydrogen in cis position with respect to OH group. From the formed *E* isomer of the enol coordinated to the catalyst the *Z* one could be formed by rotation around the C−C bond. The addition of the second water molecule to give the ketone final product occurs favorably with the support of the catalyst and involves a second hydrogen shift from oxygen to carbon. If the *E* isomer is involved, gold directly participates in the reaction, assisting the hydrogen transfer, whereas if the product is obtained starting from the *Z* isomer, gold is not directly involved. The intervention of a third water molecule lowers the energy barrier for the final elimination of a water molecule and formation of the π carbonyl bond. The theoretical insights presented in this work are expected to help us understand this gold-catalyzed hydration reaction as well as similar processes. In this perspective, work is in progress to carry out analogous calculations for the analysis of the mechanistic details of the 1,2-diphenylacetilene hydration with methanol as nucleophile.

Acknowledgment. This research has been supported by Università della Calabria. Financial support from MIUR-PRIN (2007-prot. 20077EZFR4_002) is gratefully acknowledged.

Supporting Information Available: MP2 energy profiles, selected geometrical parameters for all B3LYP- and B97-1-calculated structures of stationary points, charge distribution analysis for the $[(Ph_3P)Au\text{-alkene}]^+$ complexes, and selected geometrical parameters of B3LYP-calculated stationary points intercepted along the pathways for the outer-sphere attack of water and uncatalyzed second water molecule addition. This material is available free of charge via the Internet at http://pubs.acs.org.

References

(1) Hudrlik, P. F.; Hudrlik, A. M. In *The Chemistry of the Carbon-Carbon Triple Bond*; Patai, S., Ed.; Wiley: New York, 1978; Part 1, p 199.

(2) Schmid, G. H. In *The Chemistry of the Carbon−Carbon Triple Bond*; Patai, S., Ed.; Wiley: New York, 1978; Part 1, p 275.

(3) March, J. *Advanced Organic Chemistry*; Wiley: New York, 1992; p 762.

(4) Larock, R. C.; Leong, W. W. In *Comprehensive Organic Synthesis*; Trost, B. M., Fleming, I., Semmelhack, M. F., Eds.; Pergamon: Oxford, 1991; Vol. 4, p 269.

(5) Kozhevnikov, I. V. *Chem. Rev.* **1998**, *98*, 171–198.

(6) Drenth, W.; Hogeveen, H. *Recl. Trav. Chim. Pays-Bas* **1960**, *79*, 1002.

(7) Allen, A. D.; Chiang, Y.; Kresge, A. J.; Tidwell, T. T. *J. Org. Chem.* **1982**, *47*, 775–779, and references therein.

(8) Hinton, H. D.; Niewland, J. A. *J. Am. Chem. Soc.* **1930**, *52*, 2892–2896.

(9) Killian, D. B.; Hennion, G. F.; Niewland, J. A. *J. Am. Chem. Soc.* **1934**, *56*, 1384–1385.

(10) Hennion, G. F.; Niewland, J. A. *J. Am. Chem. Soc.* **1935**, *57*, 2006–2007.

(11) Killian, D. B.; Hennion, G. F.; Niewland, J. A. *J. Am. Chem. Soc.* **1936**, *58*, 1658–1659.

(12) Killian, D. B.; Hennion, G. F.; Niewland, J. A. *J. Am. Chem. Soc.* **1936**, *58*, 80–81.

(13) Hennion, G. F.; Murray, W. S. *J. Am. Chem. Soc.* **1942**, *64*, 1220–1222.

(14) Bassetti, M.; Floris, B. *J. Chem. Soc. Perkin Trans. 2* **1988**, 227–233.

(15) Acetaldehyde. *Ullmann's Encyclopedia of Industrial Chemistry*, 7th ed.; Wiley-VCH: Weinheim, 2006.

(16) Hintermann, L.; Labonne, A. *Synthesis* **2007**, *8*, 1121–1150.

(17) Teles, J. H.; Brode, S.; Chabanas, M. *Angew. Chem., Int. Ed.* **1998**, *37*, 1415–1418.

(18) Mizushima, E.; Sato, K.; Hayashi, T.; Tanaka, M. *Angew. Chem., Int. Ed.* **2002**, *41*, 4563–4565.

(19) Casado, R.; Contel, M.; Laguna, M.; Romero, P.; Sanz, S. *J. Am. Chem. Soc.* **2003**, *125*, 11925–11935.

(20) Roembke, P.; Schmidbaur, H.; Cronje, S.; Raubenheimer, H. *J. Mol. Catal. A.* **2004**, *212*, 35–42.

(21) Leyva, A.; Corma, A. *J. Org. Chem.* **2009**, *74*, 2067–2074.

(22) Becke, A. D. *J. Chem. Phys.* **1993**, *98*, 5648–5652.

(23) Stephens, P. J.; Devlin, F. J.; Chabalowski, C. F.; Frisch, M. J. *J. Phys. Chem.* **1994**, *98*, 11623–11627.

(24) Roithová, J.; Hrušak, J.; Schröder, D.; Schwarz, H. *Inorg. Chim. Acta* **2005**, *358*, 4287–4292.

(25) Nieto-Oberhuber, C.; López, S.; Jiménez-Núñez, E.; Echavarren, A. M. *Chem.—Eur. J.* **2006**, *12*, 5916–5923.

(26) Shi, F.-Q.; Li, X.; Xia, Y.; Zhang, L.; Yu, Z.-X. *J. Am. Chem. Soc.* **2007**, *129*, 15503–15512.

(27) Kovács, G.; Ujaque, G.; Lledós, A. *J. Am. Chem. Soc.* **2008**, *130*, 853–864.

(28) Hamprecht, F. A.; Cohen, A. J.; Tozer, D. J.; Handy, N. C. *J. Chem. Phys.* **1998**, *109*, 6264–6271.

(29) Zhao, Y.; Truhlar, D. G. *J. Chem. Theory Comput.* **2005**, *1*, 415–432.

(30) Fukui, K. *J. Phys. Chem.* **1970**, *74*, 4161–4163.

(31) Gonzalez, C.; Schlegel, H. B. *J. Chem. Phys.* **1989**, *90*, 2154–2161.

(32) Andrae, D.; Hä ussermann, U.; Dolg, M.; Stoll, H.; Preuss, H. *Theor. Chim. Acta* **1990**, *77*, 123–141.

(33) Frisch, M. J.; Trucks, G. W.; Schlegel, H. B.; Scuseria, G. E.; Robb, M. A.; Cheeseman, J. R.; Montgomery, J. A., Jr.; Vreven, T.; Kudin, K. N.; Burant, J. C.; Millam, J. M.; Iyengar, S. S.; Tomasi, J.; Barone, V.; Mennucci, B.; Cossi, M.; Scalmani, G.; Rega, N.; Petersson, G. A.; Nakatsuji, H.; Hada, M.; Ehara, M.; Toyota, K.; Fukuda, R.; Hasegawa, J.; Ishida, M.; Nakajima, T.; Honda, Y.; Kitao, O.; Nakai, H.; Klene, M.; Li, X.; Knox, J. E.; Hratchian, H. P.; Cross, J. B.; Bakken, V.; Adamo, C.; Jaramillo, J.; Gomperts, R.; Stratmann, R. E.; Yazyev, O.; Austin, A. J.; Cammi, R.; Pomelli, C.; Ochterski, J. W.; Ayala, P. Y.; Morokuma, K.; Voth, G. A.; Salvador, P.; Dannenberg, J. J.; Zakrzewski, V. G.; Dapprich, S.; Daniels, A. D.; Strain, M. C.; Farkas, O.; Malick, D. K.; Rabuck, A. D.; Raghavachari, K.; Foresman, J. B.; Ortiz, J. V.; Cui, Q.; Baboul, A. G.; Clifford, S.; Cioslowski, J.; Stefanov, B. B.; Liu, G.; Liashenko, A.; Piskorz, P.; Komaromi, I.; Martin, R. L.; Fox, D. J.; Keith, T.; Al-Laham, M. A.; Peng, C. Y.; Nanayakkara, A.; Challacombe, M.; Gill, P. M. W.; Johnson, B.; Chen, W.; Wong, M. W.; Gonzalez, C.; Pople, J. A. *Gaussian 03, revision B.05*; Gaussian, Inc.: Wallingford, CT, 2004.

(34) Cossi, M.; Rega, N.; Scalmani, G.; Barone, V. *J. Comput. Chem.* **2003**, *24*, 669–681.

(35) Hawkins, G. D.; Cramer, C. J.; Truhlar, D. G. *J. Phys. Chem. B* **1998**, *102*, 3257–3271.

(36) Jang, Y. H.; Goodard, W. A., III; Noyes, K. T.; Sowers, L. C.; Hwang, S.; Chung, D. S. *J. Phys. Chem. B* **2003**, *107*, 344–357.

(37) Orozco, M.; Luque, F. J. *J. Am. Chem. Soc.* **1995**, *117*, 1378–1386.

(38) Weigend, F.; Häser, M. *Theor. Chem. Acc.* **1997**, *97*, 331–340.

(39) Ahlrichs, R.; Bär, M.; Häser, M.; Horn, H.; Kölmel, C. *Chem. Phys. Lett.* **1989**, *162*, 165–169.

(40) Ahlrichs, R.; Bär, M.; Häser, M.; Horn, H.; Kölmel, C. *Chem. Phys. Lett.* **1998**, *294*, 143–152.

(41) Schäfer, A.; Huber, C.; Ahlrichs, R. *J. Chem. Phys.* **1994**, *100*, 5829–5835.

(42) Shapiro, N. D.; Toste, F. D. *Proc. Natl. Acad. Sci.U.S.A.* **2008**, *105*, 2779–2782.

(43) Nechaev, M. S.; Rayón, V. M.; Frenking, G. *J. Phys. Chem. A* **2004**, *108*, 3134–3142.

(44) Kim, C. K.; Lee, K. A.; Kim, C. K.; Lee, B.; Lee, H. W. *Chem. Phys. Lett.* **2004**, *391*, 321–324.

(45) Hertwig, R. H.; Koch, W.; Schröder, D.; Schwarz, H.; Hrušák, J.; Schwerdtfeger, P. *J. Phys. Chem.* **1996**, *100*, 12253–12260.

(46) Ziegler, T.; Rauk, A. *Inorg. Chem.* **1979**, *18*, 1558–1565.

(47) Dewar, M. J. S. *Bull. Soc. Chim. Fr.* **1951**, C71–C79.

(48) Chatt, J.; Duncanson, L. A. *J. Chem. Soc.* **1953**, 2939–2947.

(49) Carpenter, J. E.; Weinhold, F. *J. Mol Struct. (THEOCHEM)* **1988**, *169*, 41–62.

(50) Carpenter, J. E.; Weinhold, F. J. *The Structure of Small Molecules and Ions*; Plenum: New York, 1988.

(51) Barrows, S. E.; Eberlein, T. H. *J. Chem. Educ.* **2005**, *82*, 1329–1333.

(52) Douglas, J. E.; Rabinovitch, B. S.; Looney, F. S. *J. Chem. Phys.* **1955**, *23*, 315–323.

(53) Brown, T. J.; Dickens, M. G.; Widenhoefer, R. A. *J. Am. Chem. Soc.* **2009**, *131*, 6350–6351.

(54) Dias, H. V. R.; Wu, J. *Eur. J. Inorg. Chem.* **2008**, 509–522.

(55) Besler, B. H.; Merz, K. M., Jr.; Kollman, P. A. *J. Comput. Chem.* **1990**, *11*, 431–439.

(56) Singh, U. C.; Kollman, P. A. *J. Comput. Chem.* **1984**, *5*, 129–145.

CT100254V